M. GIZOWSKA*#, I. KOBUS*, K. PERKOWSKI*, M. PIĄTEK*, G. KONOPKA*,
I. WITOSŁAWSKA*, M. OSUCHOWSKI*

SIZE AND MORPHOLOGY OF YTTRIA NANOPOWDERS OBTAINED BY SOLUTION COMBUSTION SYNTHESIS
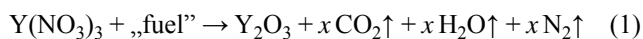
The work presents results of solution combustion method utilization for yttria (Y_2O_3) nanopowder fabrication. Experiments were carried out with four different reducing agents: urea, glycine, citric acid and malonic acid added in stoichiometric ratio. The reactions were investigated using simultaneous DSC/DTA thermal analysis. After synthesis the reaction products were calcined at temperature range of 800-1100°C and analyzed in terms of particle size, specific surface area and morphology. Best results were obtained for nanoyttria powder produced from glycine. After calcination at temperature of 1100°C the powder exhibits in a form of nanometric, globular particles of diameter <100 nm, according to SEM analysis. The d_{BET} for thus obtained powder is 104 nm, however the powder is agglomerated as the particle size measured by dynamic light scattering analysis is 1190 nm (d_{V50}).

Keywords: particle size distribution, Solution Combustion Synthesis, thermal analysis, Y_2O_3 nanopowder

1. Introduction

Yttria nanoparticles gained on interest in recent years due to unique properties of doped yttria luminescent particles. The efficiency of luminescence phenomena depends on morphology, particle size, crystallinity of the nanopowder [1-3]. Solution combustion synthesis (SCS), which is based on the high energy reaction between the metal nitrates and reducing agent, is a promising method for fabrication of nanopowders. Unlike sol-gel or precipitation technique [4,5] it is less time consuming and requires less technological steps, as the synthesis byproducts undergo thermal decomposition.

SCS method is based on redox reaction between metal nitrate and reducing agent ("fuel") giving metal oxide and non-toxic gas products. General formula of the SCS of yttria is as follows (1):

$$Y(NO_3)_3 + \text{„fuel"} \rightarrow Y_2O_3 + x\,CO_2\uparrow + x\,H_2O\uparrow + x\,N_2\uparrow \quad (1)$$

The reaction is strongly exothermic and self-propagating. The vast amounts of gas byproducts evolving during the reaction is responsible for destruction of internal structure of the produced oxide leading to fabrication of nanopowder.

First references on combustion synthesis appeared in the end of 80' [6,7] and it was used for fabrication of alumina and alumina-based mixed oxides such as: $MgAl_2O_4$, YAG, t-ZrO_2, Al_2O_3, $LaAlO_3$ and ruby powder ($Cr^{3+}:Al_2O_3$). Combustion synthesis was also utilized for fabrication of other ceramic powders, e.g.: barium titanate [8], mixed oxides for SOFC [9], superconductors [10].

In order to initiate the reaction a certain amount of energy must be supplied to the system. The initiation can be carried out in several ways:

- the reagents mixture can be conventionally heated to temperature of 400-500°C [11],
- reaction can be initiated by microwave radiation in microwave reactor or microwave oven [12].
- initiation in flame – reaction of nitrates with reducing agent is carried out simultaneously with spray pyrolysis [8,13].

An important aspect to take into account when designing a process is the choice of reagents. Depending on the type of fuel used in the synthesis following parameters varies:

- reaction initiation temperature,
- ability to create complex compound with yttrium ion in starting solution,
- amount of gaseous by-products (vast amount of gases evolved during the synthesis is supposed to break the internal structure of the obtained oxide to nanoparticles),

The literature contains examples of the use of the following compounds [6-11,14,15]: carbohydrazide, urea, amino acids (e.g. glycine, L-alanine), organic acids and saccharides.

In the presented work the relationship between the reaction path with four various reducing agents added in stoichiometric amounts and the morphology of the obtained yttria nanopowder was investigated. Following substances were used as fuel for SCS: glycine, urea, malonic acid and citric acid. The amount of gases evolved in reaction for all the fuel kinds is similar: 35 $mole_{gas}/mole_{Y2O3}$ in case of reaction with urea, and about 33 $mole_{gas}/mole_{Y2O3}$ in case of reaction of yttrium nitrate with

* INSTITUTE OF CERAMICS AND BUILDING MATERIALS, NANOTECHNOLOGY DEPARTMENT, 9 POSTĘPU STREET, 02-676 WARSAW, POLAND

Corresponding author: m.gizowska@icimb.pl

the rest of reagents. Selected reagents varied in reaction initiation temperature and in ability to create complex compound with yttrium ion in reagents solution. The initiation temperature was investigated using simultaneous differential thermal analysis. The influence of the reagents structure on the properties of the produced powder was examined basing on powders particle size, specific surface area and morphology.

2. Materials and methods

2.1. Synthesis

Yttrium nitrate hexahydrate (Sigma-Aldrich, purity 99,8%) was used for Solution Combustion Synthesis (SCS) of yttria nanopowders. Yttrium nitride was not only the precursor material for yttria synthesis, but the oxidizer in the redox reaction with reducing agent, as well. Following substances were selected for the reaction:

a) glycine (Sigma-Aldrich, purity ≥99%), b) urea (Sigma-Aldrich, purity ≥98%), c) malonic acid (Sigma-Aldrich, purity ≥99%), d) citric acid monohydrate (Sigma-Aldrich, purity ≥ 99,5%).

The synthesis was carried out according to the scheme presented in Fig. 1 [16].

The first step is dissolution of reagents for Solution Combustion Synthesis (SCS) i.e.: yttrium nitrate and reducing substance in stoichiometric amount. In this stage the reagents undergo mixing at atomic level. The solution was then heated up, so that water undergo evaporation and in case of using glycine, citric acid or malonic acid, a gel was formed. After reaching the initiation temperature, which varies according to the fuel used, high-temperature self-propagating redox reaction begins. Synthesis accompanied by glycine, citric acid and malonic acid were carried out using magnetic stirrer with conventional heating. SCS with urea were carried out in a properly modified [17] domestic microwave oven (Bosch HMT84M451, power 800 W) where the solutions were subjected to microwave radiation for 30 min.
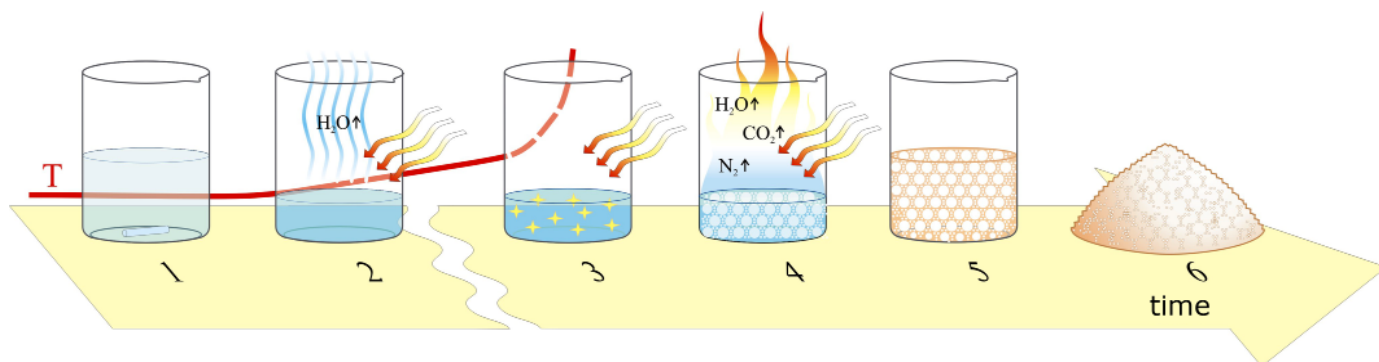

Fig. 1. Solution Combustion Synthesis of yttria nanopowder diagram; 1 – reagents solution preparation, 2 – heating of solution and evaporation of the liquid (deionized water), 3 – reaction start after achieving the initiation temperature, 4 – high-temperature, self-propagating redox reaction between yttrium nitride and fuel, 5 – reaction product i.e.: yttria nanopowder or its precursor, 6 – yttria ceramic powder [16]

2.2. Experimental

Thermogravimetric analysis was carried out using thermal analyzer TG 449 F1 Jupiter (Netzsch Gerätebau GmbH, Germany) in alumina crucibles in argon flow. The powders microstructure was characterized by means of scanning electron microscopy (Nova NanoSEM 200, FEI Company). Particle size distribution of powders aqueous suspensions was characterized by dynamic light scattering technique using zeta potential analyzer Zetasizer Nano ZS (Malvern Instruments Ltd, Worcestershire, UK). The suspensions underwent ultrasonication prior measurement (VibraCell VCX130, Sonics & Materials, Inc., Newtown, USA). The analysis results were are presented in terms of Z average (Z_{ave}, also referred as the cumulants mean or harmonic intensity averaged particle diameter) and polydispersity index (PdI) which data are intensity derived overall mean particle diameter value and overall average polydispersity. These are supported by median particle diameter (d_{V50}).

Average particle size was also calculated from specific surface area measured by BET technique (Gemini VII, Micromeritics Instrument Corp.).

3. Results and discussion

In order to investigate Solution Combustion Synthesis of yttria the solutions of reagents were analyzed using thermogravimetric technique. In Fig. 2 the mass loss (TG curves) and in Fig. 3 the detected thermal effects associated with transformations in the analyzed sample in function of temperature are presented.

Depending on the type of reducing substance the reaction proceeds according to various routs.

Thermal decomposition of yttrium nitrate ($Y(NO_3)_3 \cdot 6H_2O$) after dehydration, which takes place in few steps at temperature range of 86-350°C, undergo decomposition to oxide in two-stepped process at temperatures of about 397 and 521°C [18]. Decomposition of yttrium nitrate in presence of fuels takes place at much lower temperatures which results from the redox reaction between nitrate and the reducing substance.

With temperature increase solution of yttrium nitrate and glycine undergoes at first evaporation of water (Fig. 2a). Endothermic peaks that accompany this process are at temperature of 104 and 136°C (Fig. 3a). The first peak results from evaporation of free water from solution and the second one (with small mass
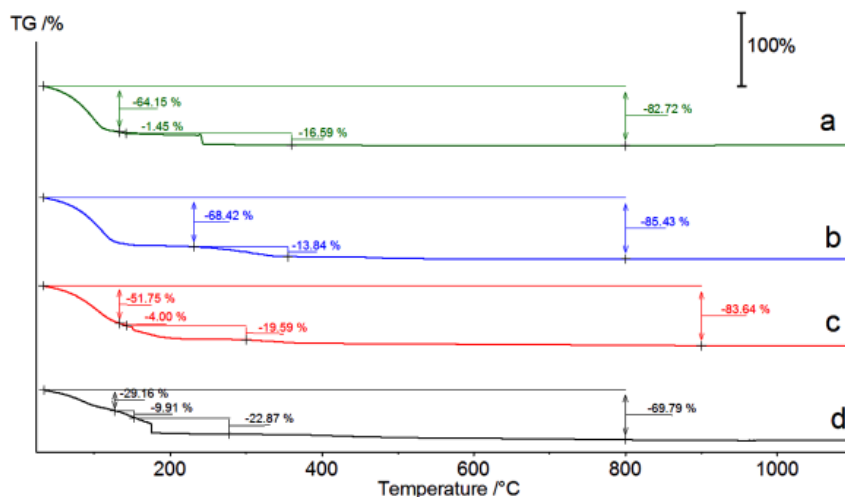
Fig. 2. TG curves of aqueous solution of yttrium nitrate and following fuels: a) glycine, b) urea, c) malonic acid, d) citric acid
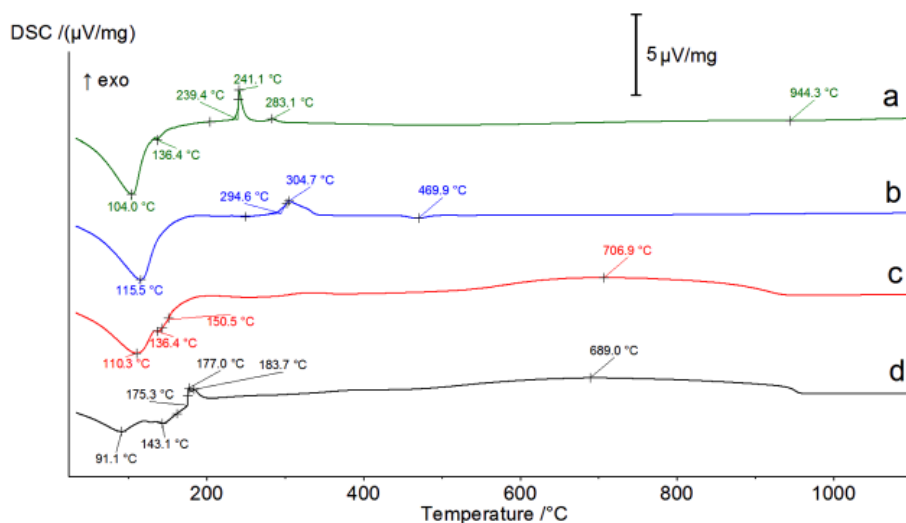

Fig. 3. DSC curves of aqueous solution of yttrium nitrate and following fuels: a) glycine, b) urea, c) malonic acid, d) citric acid

loss of about 1,45%) corresponds to removal of water from yttrium nitrate hexahydrate, which was also observed at this temperature in analysis of hydrated yttrium nitrate. At temperature of 239°C the redox reaction between yttrium nitrate and glycine begins and is accompanied by an abrupt weight loss (Fig. 2a) and sharp exothermic peak on DSC curve (Fig. 3a). Above this temperature minor weight loss is observed – 0,53% to temperature of 800°C – which indicates high conversion degree of substrates in the reaction.

Reaction of yttrium nitrate with urea starts at temperature of 294,6°C (Fig. 2b) and the exothermic peak is placed at temperature of 304,7°C (Fig. 3b). It is also preceded by water removal which ends at temperature of 175°C (Fig. 2b). The conversion to yttria is not complete as the second mass loss ($\Delta m = 3,17\%$) step can be observed above temperature of 400°C. The mass loss is accompanied by endothermic signal at temperature of 469,9°C, which indicates decompositon of $(YONO_3)_{x=1\ or\ 4}$ (an intermediate product of yttrium nitrate thermal decay [18]).

At the thermogravimetric analysis of solution containing yttrium nitrate and malonic acid two stages of water removal

can be observed with endothermic peaks at temperature of 110 and 136°C (Fig. 2c, Fig. 3c). The first stage is the evaporation of water from solution and the second results from decomposition of water built in hydrated yttrium nitrate crystal. Redox reaction starts at temperature of 150,5°C, the effect of DSC curve is not distinct, but at TG curve sharp slope of mass loss can be observed. The reaction is not complete as further mass loss is observed above temperature of 300°C ($\Delta m = 8,30\%$).

Removal of water in yttrium nitrate – citric acid system proceeds similarly as in previous nitrate – malonic acid system – in two stages giving endothermic peaks at temperatures of 91,1 and 143,1°C. Reaction between citric acid and yttrium nitrate starts already at temperature of 175,3°C giving very sharp exothermic signal on DSC curve ($T_{max.\ peak} = 177$ and 183,7°C, Fig. 3d) and an abrupt weight loss (Fig. 2d). However, the reaction energy must be not sufficient for total conversion to yttria as further mass loss above 300°C can be observed ($\Delta m = 7,85\ \%$).

The synthesis of yttria was carried out with the selected fuels added in stoichiometric amounts according to scheme presented in Fig. 1. Calcination of the produced powders is indispensable

as in all cases mass loss after reaction was observed. Calcination temperature was selected basing on the results of thermal analysis – it was the temperature at which no significant mass loss was observed. Yttria precursors obtained from reaction with glycine, urea and citric acid were calcined at temperature of 800°C and one obtained from reaction with malonic acid was calcined at temperature of 900°C. Additionally, all powders were calcined at temperature of 1100°C. The particle size of the synthesized powders were measured using dynamic laser scattering (dls) technique and calculated from BET surface. The results are presented in Table 1.

From the results presented in Table 1 significant difference between the particle diameter measured by dynamic light scattering and BET method can be noticed. From the measurements of powder diameter in suspension (dls method) it can be concluded that the synthesized powders are of micrometric size, whereas, the BET measurements prove that the powder have a developed surface suggesting nano- or submicrometric particle size. The SEM micrographs of the calcined powders presented in Fig. 4-7 reveal the reason of these discrepancies. The powders obtained

TABLE 1

Particle size measured by dynamic light scattering (dls) method and calculated from BET surface of yttria powders obtained by SCS method (Z_{ave} – cumulant mean, PdI – polydispersity index, d_{V50} – median diameter of the particle size distribution measured by dls method, S_{BET} – specific surface area measured by BET mehtod, d_{BET} – BET equivalent spherical particle diameter)

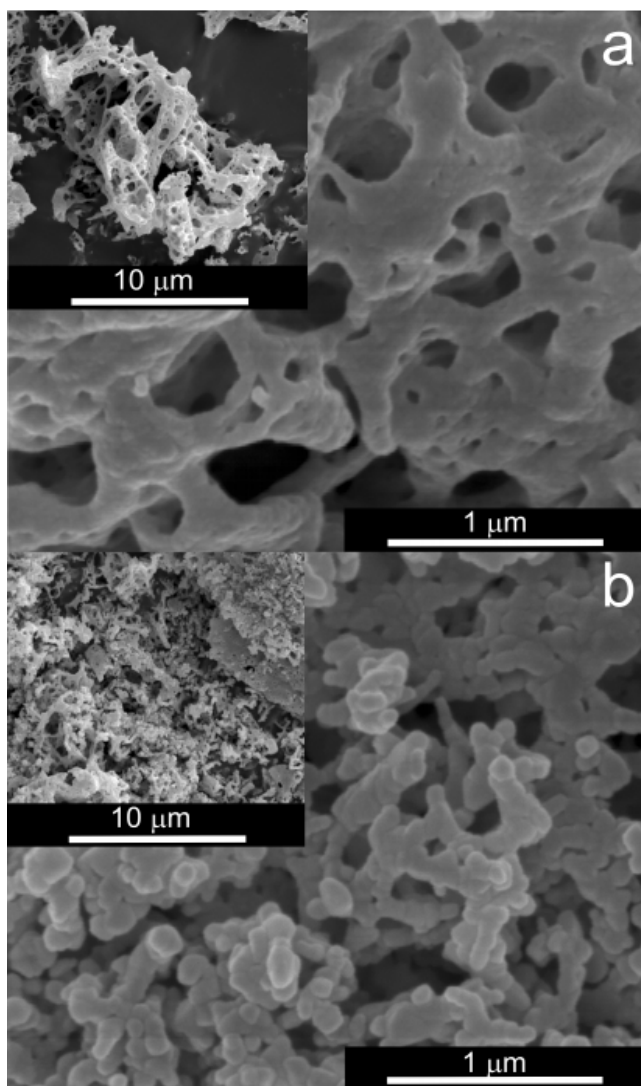| Type of fuel used in the synthesis	Calcination temperature, °C	Z_{ave}, nm	PdI	d_{V50}, nm	S_{BET}, m²/g	d_{BET}, nm
Glycine	800	2694	0,74	859	19,7	61
	1100	1338	0,37	1190	11,5	104
Urea	800	2207	0,36	1790	20,9	57
	1100	870	0,42	759	9,2	130
Malonic acid	900	3082	0,94	944	4,2	285
	1100	951	0,52	784	9,5	126
Citric acid	800	2043	0,60	1050	13,2	91
	1100	1095	0,56	925	5,9	202

Fig. 4. Micrographs of yttria nanopowder obtained by SCS reaction with glycine calcined at temperature of: a) 800°C and b) 1100°C
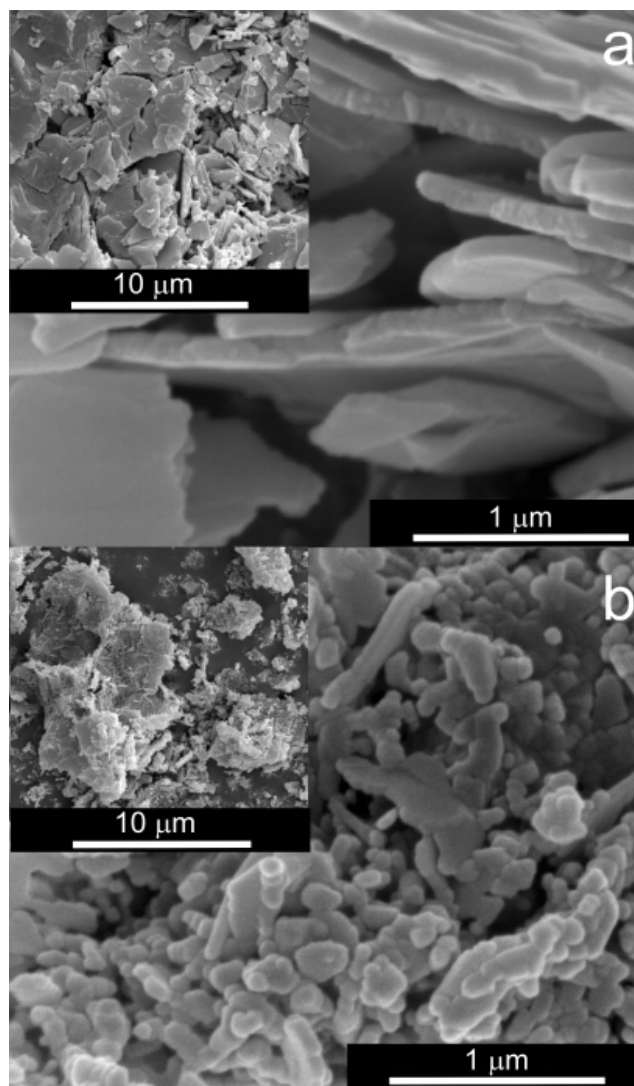

Fig. 5. Micrographs of yttria nanopowder obtained by SCS reaction with urea calcined at temperature of: a) 800°C and b) 1100°C

in the synthesis occur in agglomerates and aggregates consisting of nanostructures.

Reaction of yttrium nitrate with glycine lead to fabrication of Y_2O_3 powder characterized highly porous microstructure. Powders calcined at temperature of 800°C have sponge-like structure (Fig. 4a). The dls analysis provides information about average particle size. Cumulant mean is: $Z_{ave} = 2,7$ μm while $d_{V50} = 0,9$ μm. High value of Z_{ave} indicates presence of much larger particles – larger than the range taken for distribution analysis, which is also expressed in high polydispersity index. The aggregates are also visible in SEM analysis (Fig. 4a). The BET surface is 19,7 m²/g demonstrating relatively highly developed surface. Calcination at temperature of 1100°C cause structure change with no mass loss (Fig. 2a). In thus prepared powder globular particles of about 100 nm in diameter are visible (Fig. 4b), the agglomerates size (measured by dls method) decrease to $Z_{ave} = 1,3$ μm and $d_{V50} = 1,2$ μm, but BET surface decrease as well and equals 11,5 m²/g (Table 1). During calcination at temperature of 1100°C the disordered matter in nanostructures of high surface energy undergo diffusion and organization in grains. The "sponge-like"

structure undergoes conversion – its thin walls disappear and on its place the uniform globular grains are produced. The specific surface decreases in the process of matter diffusion and forming of grains, but the globular grains are connected by van der Waals forces or sintering necks. Such structure is more probable to undergo disintegration than the primal "sponge-like" aggregates which is expressed in dls analysis. Mild exothermic effect on DSC curve at temperature of about 900°C, indicates sintering process and related with it decrease of surface energy.

Reaction of yttrium nitrate with urea leads to production of powder of platelet-like shape (Fig. 5a), which are present in water suspension as agglomerates of diameter: $Z_{ave} = 1,2$ μm. The specific surface area is very high and equals 20,9 m²/g. After calcination at temperature of 1100°C nanosized grains are revealed (Fig. 5b), however, the measured agglomerate size is only slightly lower and equals: $Z_{ave} = 0,9$ μm and $d_{V50} = 0,8$ μm.

Powders produced with malonic are characterized by porous structure (Fig. 6). After calcination at temperature of 900°C particle size of yttria powder is $Z_{ave} = 3,1$ μm and $d_{V50} = 0,9$ μm. Specific surface area is relatively low in comparison with other
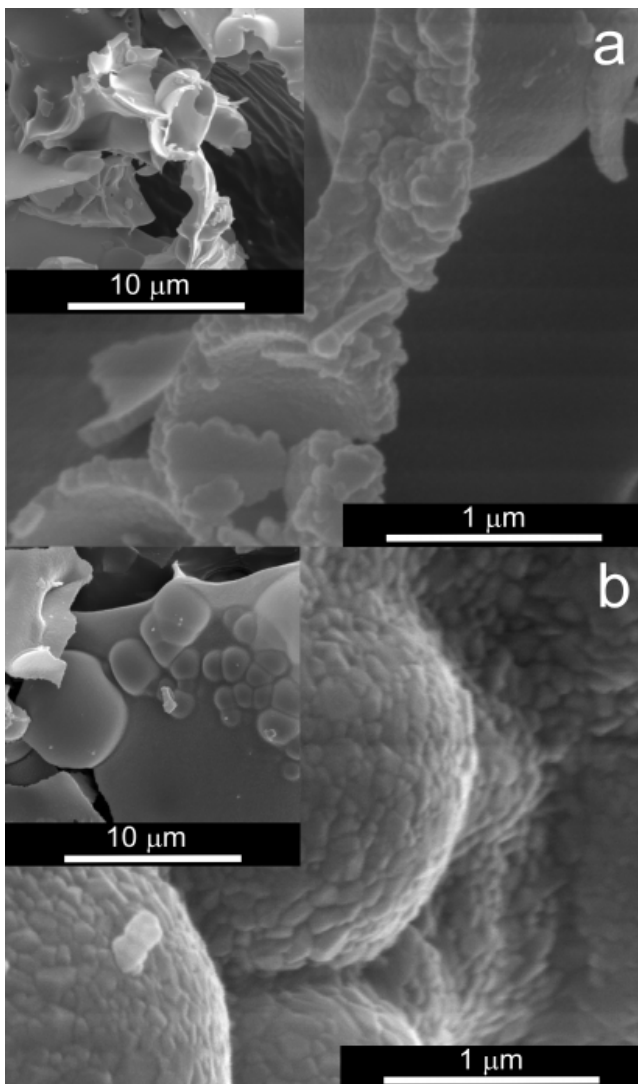

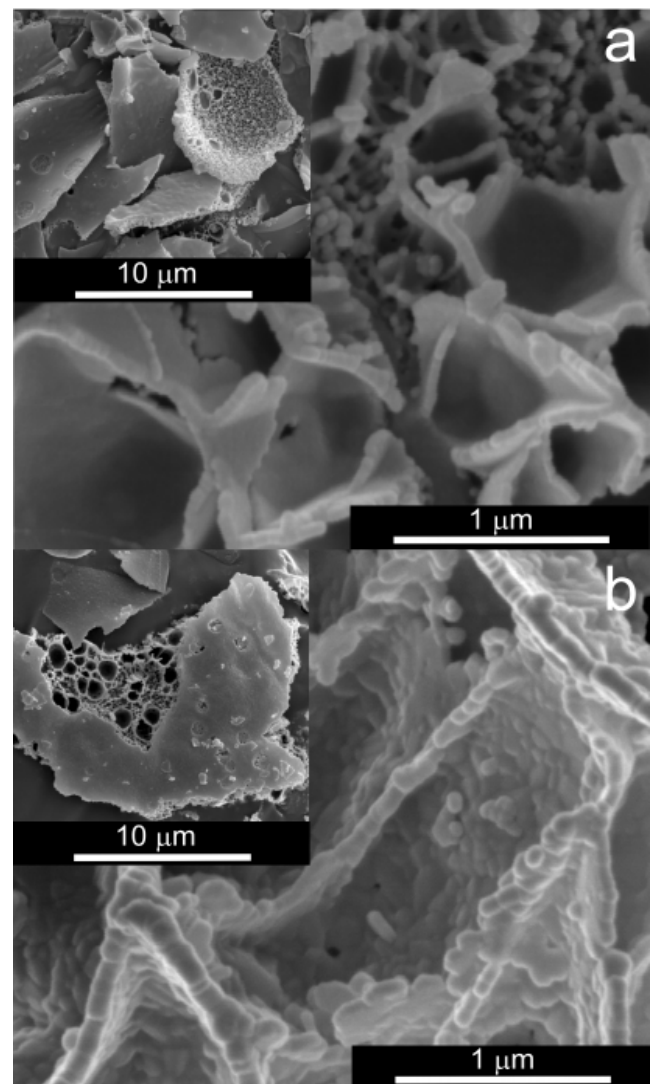Fig. 6. Micrographs of yttria nanopowder obtained by SCS reaction with malonic acid calcined at temperature of: a) 900°C and b) 1100°C

Fig. 7. Micrographs of yttria nanopowder obtained by SCS reaction with citric acid calcined at temperature of: a) 800 C and b) 1100°C

powders produced by SCS and equals 4,2 m²/g. After calcination at temperature of 1100°C particle size decreases: Z_{ave} = 1,0 μm and d_{V50} = 0,5 μm (Table 1). Interestingly, specific surface area increased indicating partial destruction of the aggregates and nanostructurization of powder.

Morphology of yttria powder produced in reaction with citric acid (Fig. 7) is similar to one produced with malonic acid. Particle size of yttria powder obtained from synthesis using citric acid is Z_{ave} = 2,0 μm and d_{V50} = 1,1 μm. Specific surface area is 13,2 m²/g suggesting nanosized powder. After calcination at temperature of 1100°C size of agglomerates in the powder decreases (Z_{ave} = 1,1 μm and d_{V50} = 0,9 μm), however the grains undergo sintering as the specific surface area is much lower (S_{BET} = 5,9 m²/g).

4. Conclusions

- According to thermogravimetric data together with observation of microstructure the Solution Combustion Synthesis SCS of yttria proceeds in following steps: 1 – evaporation of water accompanied by endothermic effect on DSC curve and mass loss on TG, 2 – redox reaction observed as exothermic peak on DSC and in some cases very rapid mass loss, 3 – thermal decomposition of reaction residues, 4 – sintering or reorganization of matter in nanopowder accompanied by mild exothermic effect with no mass loss.
- Solution Combustion Synthesis (SCS) can be successfully utilized for fabrication of yttria nanopowder using glycine, urea, malonic acid or citric acid as a reducing substance.
- Depending on the "fuel" type used in the SCS powders of different microstructure were obtained. This suggests that the molecular structure of the fuel has significant impact on the reaction path and formation of the yttria powder. Using substances which can create complex compound with yttrium ion in the starting solution (i.e. glycine, citric acid, malonic acid) spacious structures. In contrast, reaction with urea, which does not show affinity to metal ions in solution and has flat conformation, leads to fabrication of platelet-like structured yttria powders.
- Reaction of yttrium nitrate with glycine, urea, malonic acid and citric acid takes place beneath 300°C, the ignition temperature is respectively: 239, 294,6, 150,5, 175,3°C. In all cases produced powders must be calcined in order to burnout substrate residues. The burnout takes place up to temperature of 800°C for product of reaction with glycine, urea and citric acid, in case of using malonic acid, the burnout takes place in temperature of 900°C.
- Calcination at higher temperature (1100°C) causes in most cases decrease in specific surface in result of sintering of the material. The exception is powder produced with malonic acid in which the BET surface increases twice (S_{BET}(900°C) = 4,2 m²/g, S_{BET}(1100°C) = 9,5 m²/g), however the reasons for such behavior is not yet known and will be subject for further studies.

- The process of sintering (during calcination at temperature of 1100°C) causes degradation of the primal structure of the produced powders, which is most visible in case of powders produced with glycine and urea. The "sponge-like" structure of glycine derived powder and platelets formed in reaction with urea undergo restructuration to agglomerates built from globular nanograins (according to SEM analysis d < 100 nm). The agglomerates diameter (d_{V50}) measured by dls method is respectively: 1190 and 759 nm.

REFERENCES

[1] Y.C. Kang, I.W. Lenngoro, S.B. Park, K. Okuyama, Mater. Res. Bull. **35**, 789-798 (2000).

[2] H. Chang, I.W. Lenggoro, K. Okuyama, T.O. Kim, Jpn. J. Appl. Phys. **43**, 3535 (2004).

[3] S.K. Lee, H.H. Yoon, S.J. Park, K.H. Kim, H.W. Choi, J. J. Appl. Phys. **46**, 7983-7986 (2007).

[4] K. Serivalsatit, B. Kokuoz, B. Yazgan-Kokuoz, M. Kennedy, J. Ballato, J. Am. Ceram. Soc. **93** (5), 1320-1325 (2010).

[5] R. Mellado-Vázquez, M. García-Hernández, A. López-Marure, P.Y. López-Camacho, Á.J. Morales-Ramírez, H.I. Beltrán-Conde, Materials **7**, 6768-6778 (2014).

[6] J.J.Kingsley, K.C. Patil, Mater. Lett. **6** (11), 427-432 (1988).

[7] J.J. Kingsley, K. Suresh, K.C. Patil, J. Solid State Chem. **88** (2), 435-442 (1990).

[8] Y. Terashi, A. Purwanto, W. Wang, F. Iskandar, K. Okuyama, J. Eur. Ceram. Soc. **28**, 2573-2580 (2008).

[9] Z. Shao, W. Zhou, Z. Zhu, Prog. Mater. Sci. **57**, 804-874 (2012).

[10] M.S.M. Suan, M.R. Johan, T.C. Siang, Physica C **480**, 75-78 (2012).

[11] R.V. Mangalaraja, J. Mouzon, P. Hedström, I. Kero, K.V.S. Ramam, C.P. Camurri, M. Od´en, J. Mater. Process. Technol. **208,** 415-422 (2008).

[12] K. Laishram, R. Mann, N. Malhan, Powder Technol. **229**, 148-151 (2012).

[13] F. Iskandar, Adv. Powder Technol. **20**, 283-292 (2009).

[14] W. M. Yen, M. J. Weber, CRC Press, 22.06.2004.

[15] A. Dupont, C. Parent, B. Le Garrec, J.M. Heintz, J. Solid State Chem. **171**, 152-160 (2003).

[16] M. Gizowska, I. Kobus, K. Perkowski, M. Zalewska, G. Konopka, I. Witosławska, M. Osuchowski, K. Jakubiuk, A. Witek, Szkło i Ceramika **5**, 23-26 (2016).

[17] I. Kamińska, Nanostruktury tlenkowe domieszkowane lantanowcami lub metalami przejściowymi do obrazowania biomedycznego, dissertation, Środowiskowe Laboratorium Fizyki Biologicznej, Instytut Fizyki Polskiej Akademii Nauk, Warszawa 2016.

[18] P. Melnikov, V.A. Nascimento, L.Z.Z. Consolo, A.F. Silva, J. Therm. Anal. Calorim. **111**, 115-119 (2013).